

## Cartilage mechanics in the guinea pig model of osteoarthritis studied with an osmotic loading method

Charlene M. Flahiff†, Virginia B. Kraus‡, Janet L. Huebner‡ and Lori A. Setton†\*

† Department of Biomedical Engineering, Duke University, Durham, NC, USA

‡ Department of Medicine, Division of Rheumatology, Allergy, & Clinical Immunology, Duke University Medical Center, Durham, NC, USA

### Summary

**Objective:** To determine the material properties of articular cartilage in the Hartley guinea pig model of spontaneous osteoarthritis.

**Methods:** Cartilage-bone samples from the medial femoral condyle and tibial plateau of 12 month-old guinea pig knees were subjected to osmotic loading. Site-matched swelling strains and fixed charge density values were used in a triphasic theoretical model for cartilage swelling to determine the modulus of the cartilage solid matrix. The degree of cartilage degeneration was assessed in adjacent tissue sections using a semi-quantitative histological grading scheme.

**Results:** Decreased values for both moduli and surface zone fixed charge density were associated with increasing grades of cartilage degeneration. Decreases in moduli reflect damage to the collagen matrix, which give rise to greater swelling strains.

**Conclusion:** Histological evidence of cartilage degeneration was associated with impaired cartilage mechanics in the aging Hartley guinea pig.

© 2004 OsteoArthritis Research Society International. Published by Elsevier Ltd. All rights reserved.

The Hartley guinea pig develops osteoarthritis (OA) naturally and displays progressive degenerative changes that closely resemble the development of OA in humans. In this model of OA, degenerative changes begin to develop on the medial tibial plateau as early as 3 months of age and progress to a moderate or severe stage by 12 months<sup>1–4</sup>. The histological and biochemical features of OA observed in this animal model that are similar to those seen in the human include hypocellularity, proteoglycan loss, surface fibrillation, osteophyte formation, and expression of collagenases in degrading cartilage<sup>2,3,5–8</sup>. Thus, the Hartley guinea pig is an attractive animal model with relevance to cartilage degeneration in humans. Although histological and biochemical features of OA have been well documented in this animal model, to date no information is available on corresponding changes in the mechanical properties of guinea pig cartilage with degeneration.

Previous studies of human articular cartilage and of experimental models of OA have shown that the tensile stiffness, as well as the shear moduli, decreases in tissue that is fibrillated or osteoarthritic<sup>9–17</sup>. The decrease in material stiffness with degeneration is believed to be related to a ‘weakening’ of the collagen fibrillar network, which may affect the cartilage contribution to load support and distribution during joint loading and motion. While measures of cartilage mechanics have not been obtained for the guinea pig, the increased surface fibrillation<sup>2</sup> and collagenase expression demonstrated in this guinea pig

model of OA<sup>8</sup> suggest that corresponding decreases in tensile stiffness may occur for guinea pig cartilage.

Mechanical testing in small animal joints, including the guinea pig, poses difficulties with preparing and gripping small cartilage test specimens, where cartilage thickness is typically less than 500 microns. Thus, few mechanical studies have been performed previously on cartilage from small animal joints. An alternative to conventional material testing methods is offered by osmotic loading. Osmotic loading exploits the intrinsic swelling propensity of cartilage and has been shown to be useful for quantifying stiffness of the cartilage matrix<sup>18,19</sup>. Swelling effects in cartilage arise from the presence of negatively-charged glycosaminoglycans, which generate a large interstitial osmotic pressure that is restrained by elastic forces in the collagen network<sup>20,21</sup>. Thus, the amount of cartilage swelling in an osmotically active solution reflects a balance between the interstitial swelling pressure and the mechanical integrity, or stiffness, of the cartilage matrix.

Previously, we developed a method to quantify the mechanical properties of human and canine knee articular cartilage from the swelling behavior in osmotically active solution. The cartilage matrix uniaxial modulus was determined from experimental measures of swelling strain using a triphasic theoretical formulation of cartilage in the free-swelling configuration<sup>22</sup>. Using this technique, moduli were found to compare well with tensile moduli of site-matched tissue determined in a conventional simple tension test<sup>22</sup>. We recently modified the osmotic loading method to quantify cartilage mechanics in the guinea pig knee<sup>23</sup>. Values for the moduli of non-degenerate guinea pig cartilage compared favorably with those of non-degenerate human and canine cartilages<sup>22–24</sup>.

\*Address correspondence to: Lori A. Setton, Ph.D., Duke University, Department of Biomedical Engineering, 136 Hudson Hall, Box 90281, Durham, NC 27708, USA. Tel: +1 919-660-5131; Fax: +1 919-660-5362; E-mail: setton@duke.edu

Received 9 July 2002; revision accepted 24 January 2004.

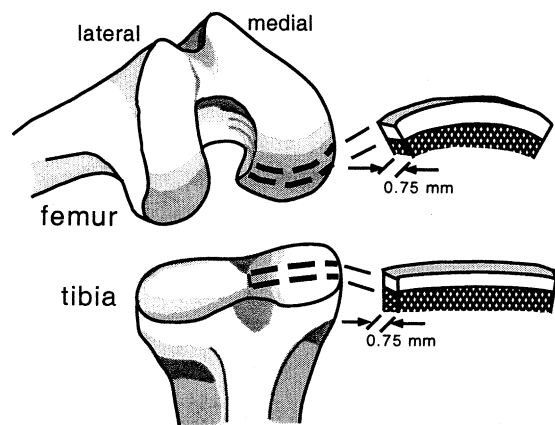


Fig. 1. Schematic of specimen preparation. Cartilage-bone samples of 0.75 mm thickness were used for strain analysis. Histology was obtained for semi-quantitative histochemical analysis.

In this study, we used osmotic loading to quantify cartilage mechanics in the knees of 12 month-old Hartley guinea pigs with established histological OA. We hypothesized that histological evidence of cartilage damage in the joints of the skeletally mature Hartley guinea pig is associated with decreases in the uniaxial modulus, reflecting a decrease in tensile stiffness of the cartilage solid matrix. Since these guinea pigs undergo spontaneous cartilage degeneration with age, this study provides useful and novel information on variability in cartilage function and pathology in a naturally-occurring degenerative process.

## Methods

Twenty-five explant samples ( $n=5$ , femur;  $n=20$ , tibia) of cartilage and underlying bone (cartilage-bone) were prepared from the medial compartment of 12 month-old male Hartley guinea pig knees (Charles River Labs), as described previously<sup>23</sup>. All animals were obtained through a protocol approved by the Institutional Animal Care and Use Committee. Either the medial femoral condyle or medial tibial plateau was obtained from each animal and sectioned transverse to the cartilage-bone interface to obtain flat, 0.75 mm thick, planar sections of cartilage-bone (Fig. 1). The central third of each compartment was used for strain analysis, semi-quantitative histochemical analysis, and histological grading.

For free-swelling tests, nuclei of cartilage and bone cells were fluorescently labeled and visualized using confocal laser scanning microscopy as described previously<sup>23</sup>. The bone nuclei served as fixed markers, while cartilage nuclei served as strain markers. Since swelling effects in cartilage are negligible at hypertonic ion concentrations due to the shielding of negatively charged proteoglycans<sup>21,25</sup>, a zero stress-strain reference configuration was chosen at 2 M NaCl. Samples were equilibrated in the hypertonic reference solution for 1 h. High resolution planar images of the cartilage-bone sample were obtained as a reference image (Fig. 2). Samples were then equilibrated in a hypotonic solution (0.015 M NaCl) for 1 h, and corresponding images of the swollen state were recorded.

Image analysis was performed to calculate the swelling-induced strain throughout the cartilage layer, as described previously<sup>19,23</sup>. Briefly, triads of cartilage markers were

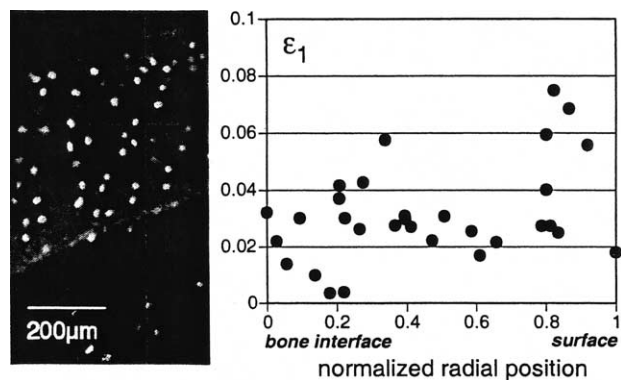


Fig. 2. A representative image of a guinea pig cartilage-bone sample from the tibial plateau, showing fluorescently labeled bone and cartilage nuclei (left); and a plot of strain,  $\epsilon_1$ , versus normalized radial position for a representative tibial sample (right).

defined, and the spatially varying, two-dimensional components of Lagrangian strain  $E_{ij}$  ( $i,j=r,\theta$ ) were calculated for each triad from images recorded at the swollen state, with respect to the hypertonic reference state (Fig. 2). Corresponding components of infinitesimal strain were calculated from the measured swelling strains, and the principal swelling strains were calculated for use in the theoretical model.

Theoretical predictions of the swelling strain in cartilage depend upon the proteoglycan-associated fixed charge density of the tissue. A semi-quantitative histochemical technique was used to determine the non-uniform fixed charge density of the cartilage matrix from the red intensity of safranin O, a stain shown to correlate highly with fixed charge density<sup>26</sup>. For our calibration procedure in this study, human patellar cartilage samples ( $n=48$ ) were used to correlate biochemical measures of fixed charge density with red intensity of safranin O stain using methods described previously<sup>23</sup>. All samples were routinely prepared for histology, sectioned to a thickness of 5 μm, and stained with safranin O<sup>27</sup>. High resolution RGB images of the histological sections were obtained using a slide scanner (Polaroid, SprintScan 35 Plus, 2700 dpi resolution) with the same settings used for all image acquisitions. The intensity of safranin O (red content) was determined throughout the depth of the cartilage layer from the digitized images pixel-by-pixel<sup>23</sup>, based on a modification of methods developed by Martin *et al.*<sup>28</sup>. Red intensity values,  $R_c$ , for human cartilage were plotted against measured fixed charge density ( $c_0^F$ ) in site-matched samples<sup>23</sup>, and a single exponential term was numerically fit to the data to obtain calibration constants, A and B, from the equation,  $c_0^F = A(\exp(B \cdot R_c) - 1)$  mEq/ml tissue water. Fitted values yielded a high correlation between biochemical data and digitized image data (Fig. 3,  $A=0.00269$  mEq/ml tissue water,  $B=0.0821$ ;  $r=0.87$ ). This equation and calibration constants were then used to convert red intensity values ( $R_c$ ) for guinea pig cartilage, stained with safranin O and analyzed as described above, to reference fixed charge density ( $c_0^F$ ) as a function of depth. The depth-dependent fixed charge density values obtained for each guinea pig sample were grouped by zone to correspond to the surface (upper 25%), middle (33–75%), and deep zones (lower 33%) of articular cartilage. In addition, a thickness-averaged fixed charge density was calculated. Repeated tests on adjacent samples has shown the precision error in this technique to be 0.016 mEq/ml tissue water ( $n=22$ ).

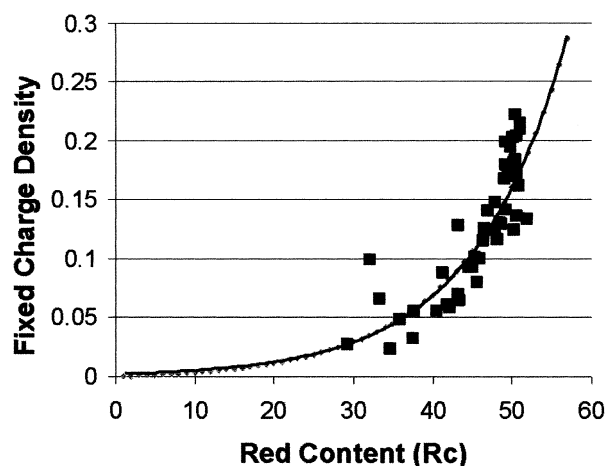


Fig. 3. Non-linear regression of biochemical data for human cartilage on corresponding digitized image data (Rc) using the equation,  $c_0^F = A[\exp(B \cdot Rc) - 1]$  mEq/ml tissue water ( $A=0.00269$ ,  $B=0.0821$ ;  $r^2=0.75$ ).

To determine the uniaxial modulus, a triphasic model for cartilage swelling<sup>21,24,29</sup> was used to predict the magnitude and distribution of swelling-induced strains for each sample. Free-swelling of the cartilage layer was modeled for equilibration against an external hypotonic bath (0.015 M NaCl), and the components of infinitesimal strain due to swelling were predicted relative to the hypertonic reference configuration (2 M NaCl)<sup>22</sup>. In this model, the cartilage solid matrix was assumed to have homogeneous material properties (i.e. uniaxial modulus) and spatially-varying fixed charge density, which were obtained using histochemical analysis as described above. Constant values for reference water volume fraction (0.8, hypertonic reference state), thickness to radius of curvature (1:7), and Poisson's ratio (0.25)<sup>30</sup> were chosen as described previously<sup>23,24</sup>. Thus, predictions for swelling-induced strain reduced to a dependence on one parameter, the uniaxial modulus. Model predictions for swelling were matched to experimental measures of the principal swelling strains to obtain the uniaxial modulus.

For histological grading, sections from each sample were stained with safranin O/fast green<sup>27</sup> and were independently graded by two blinded investigators to assess cartilage degeneration in the same region studied in the swelling test. A modified semi-quantitative grading scheme was used, based on the work of Mankin and co-workers and Carlson and co-workers<sup>31,32</sup>, but adapted for the guinea pig<sup>33</sup>. This grading scheme consisted of gross assessment of the cartilage structure (scale=0–8: 0=normal, smooth cartilage surface; 8=clefts extending throughout the deep zone) and proteoglycan staining (scale=0–6: 0=uniform, staining throughout the cartilage; 6=over 50% reduced staining in all three zones)<sup>33</sup>. Thus, the minimum score in each category corresponded to normal cartilage, while the maximum score reflected severe degeneration. The two scores for each sample were also added together to obtain a total histological grade representing chondropathy (scale=0–14). This grading scheme has been shown to accurately reflect histological changes in the knee joints of the guinea pig that correlate significantly to biomarkers of osteoarthritic disease<sup>33</sup>.

A one-factor analysis of variance (ANOVA) was used to detect a difference in the uniaxial modulus and

Table 1  
Uniaxial modulus and thickness-averaged fixed charge density ( $c_0^F$ ) for femoral and tibial cartilage

	Uniaxial modulus (MPa)	$C_0^F$ (mEq/ml water)
Femoral condyle	10.2±4.4, n=3	0.093±0.032, n=3
Tibial plateau	10.1±7.1, n=19	0.101±0.040, n=20

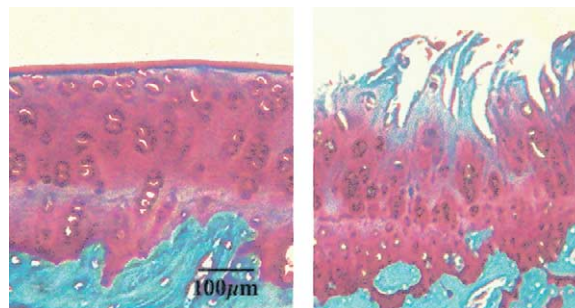


Fig. 4. Histological images (10x) showing varying states of cartilage degeneration. A femoral section (left) shows mild cartilage degeneration, characterized by dark, uniform staining and mild surface irregularities, while a tibial section (right) shows severe cartilage degeneration, characterized by substantially reduced staining and extensive cartilage fibrillation.

thickness-averaged fixed charge density between femoral and tibial cartilage. A one-factor ANOVA and Student–Newman–Keuls (SNK) post-hoc test using repeated measures were performed to test for a difference in fixed charge density values among cartilage zones. Non-parametric methods (Mann–Whitney) were used to compare histological grades of femur and tibia and to calculate the correlation coefficients (Spearman) for histological grade against both uniaxial modulus and zonal fixed charge density. Results at a level of  $P < 0.05$  were considered significant.

## Results

Insufficient strain measurements prevented moduli determination for one tibial sample, and insufficient sample size for safranin O staining prevented fixed charge density measurements in two femoral samples. The uniaxial modulus and thickness-averaged fixed charge density values were similar for tibial and femoral cartilage with average values of 10.1±6.7 MPa and 0.106±0.041 mEq/ml tissue water for all samples (Table 1). The fixed charge density values were lowest in the surface zone of cartilage for both the tibia and the femur; however, this finding was significant only for the tibial cartilage ( $P < 0.05$ , SNK:  $c_0^F = 0.049 \pm 0.036$ , surface;  $0.120 \pm 0.049$ , middle;  $0.113 \pm 0.040$  mEq/ml tissue water, deep).

Cartilage from both the femurs and tibiae of 12 month-old guinea pig knee joints exhibited varying states of degeneration, from very mild degeneration with uniform proteoglycan staining and few surface irregularities to severe degeneration, indicated by substantially reduced staining and extensive cartilage fibrillation (Fig. 4). The femoral samples generally showed only mild degeneration, while most of the tibial samples showed moderate to severe degeneration. Loss of staining was similar in tibial and femoral cartilage, while cartilage structural abnormalities were more severe in the tibia (Fig. 5).

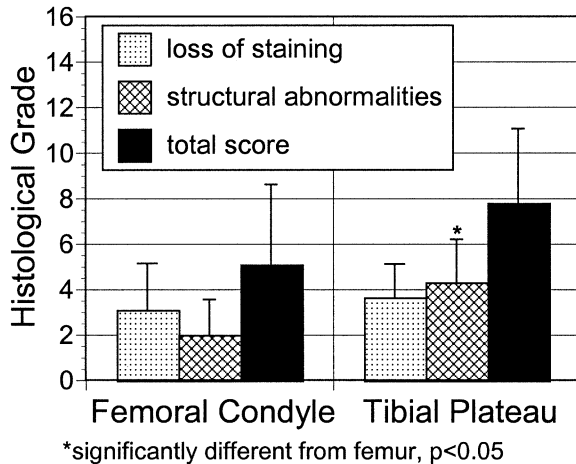


Fig. 5. Proteoglycan staining, structural abnormalities, and total histological grades are shown for femoral and tibial cartilage. Cartilage structural abnormalities were significantly greater in the tibia than in the femur.

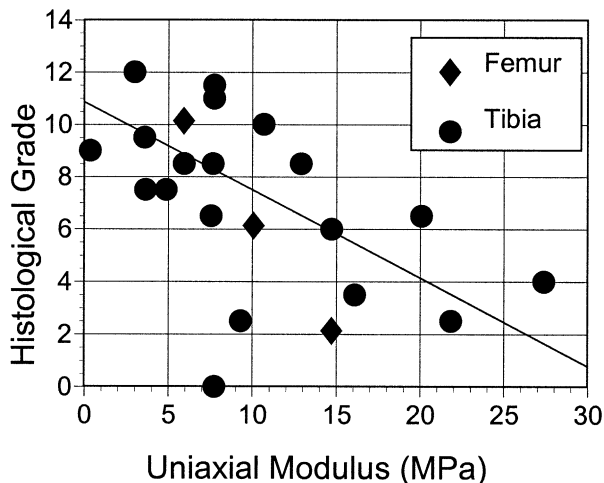


Fig. 6. Total histological grade versus uniaxial modulus for tibial and femoral samples. A negative correlation between histological grade and uniaxial modulus was detected ( $r=-0.57$ ,  $P<0.006$ ).

There was evidence of a moderate correlation between total histological grade and the uniaxial modulus for all samples ( $r=-0.57$ ,  $P<0.01$ ). With increasing histological grade of cartilage degeneration, the value for the uniaxial modulus decreased (Fig. 6). Looking at femur and tibia independently, this correlation was significant in the tibia ( $r=-0.53$ ,  $P=0.03$ ), but not in the femur ( $r=-0.90$ ,  $P=0.16$ ), although the trend was similar. There was also a significant and negative correlation between total histological grade and surface zone fixed charge density ( $r=-0.65$ ,  $P=0.002$ ) for all samples. Looking at femur and tibia separately, this correlation was only significant in the tibia ( $r=-0.53$ ,  $P=0.02$ ).

## Discussion

In this study, the material properties of Hartley guinea pig cartilage were quantified using an osmotic loading method to evaluate changes in cartilage mechanics associated with the natural development of OA in this animal model.

Osteoarthritic changes were more severe in the tibia than the femur, which is entirely consistent with previous studies showing that the medial tibial plateau is the site of OA initiation in the Hartley guinea pig model<sup>1-4</sup>. Variability in the extent and location of cartilage degeneration clearly contributed to the variability seen in the values of material properties for guinea pig cartilage. Nevertheless, moduli values obtained here with the osmotic loading method are similar to those previously reported for human and canine cartilages, determined either in simple tension<sup>10-12,16</sup> or with osmotic loading<sup>22,24</sup>. Importantly, decreases in material moduli were observed with increasing grades of degeneration, exhibiting a pattern that is well-established for human OA cartilage<sup>10,34,35</sup>. Decreases in the material moduli likely reflect damage to the collagen matrix, resulting in greater swelling strains and more compliant tissue. The noted association of cartilage moduli with degenerative grade demonstrates that this osmotic loading method can provide a way to detect changes in cartilage matrix integrity with cartilage damage and OA in small animal joints such as the guinea pig.

Mechanical testing of cartilage in the guinea pig is complicated by the small quantities of available tissue. Recently, investigators have developed methods to evaluate the compressive behavior of cartilage in small animal joints, such as rats<sup>30</sup> and mice<sup>36</sup> using an *in situ* indentation test. The material properties obtained for rat cartilage were shown to be consistent with those of larger animal joints. The mechanical behaviors of cartilage in compression, however, are believed to depend largely on the contents of proteoglycan and water and thus, are not likely to be sensitive to changes in the collagen molecular network. Osmotic loading provides a way to determine a modulus that reflects the tensile properties, as shown in our previous work comparing uniaxial moduli and tensile moduli of site-matched tissues<sup>22</sup>. The advantages of osmotic loading include an ability to leave the cartilage on the subchondral bone and the absence of grips or platens to clamp the sample, which makes this technique particularly useful for studying cartilage mechanics when sample size is limiting, such as in rodent model systems. Use of the osmotic loading method depends on knowledge of the fixed charge density, however, which is challenging to obtain in small tissue samples using biochemical assays. Thus, it was necessary to develop a quantitative histochemical method to quantify fixed charge density in the guinea pig samples studied here. The full-thickness values for fixed charge density obtained here with this new method are consistent with reported values for other species obtained using biochemical measures<sup>19,22</sup>.

In a previous study of human articular cartilage, increases in histological evidence of OA were coincident with loss of tensile stiffness at the surface zone and correlated strongly with depth of the surface zone region<sup>22</sup>. These findings provided quantitative support for the hypothesis that impaired function associated with OA initiates at the surface zone, which may contribute to the progression of disease. In the current study of the guinea pig cartilage, although data were available for zonal variations in fixed charge density, the thin cartilage layer in the guinea pig precluded measures of the non-uniform swelling strain fields essential for determining zonally-varying material properties. Nevertheless, fixed charge density at the surface zone of cartilage was found to correlate with the histological severity of cartilage degeneration. This finding suggests that the biochemical changes associated with OA may initiate at the surface zone. Modification of the method

to permit determinations of the moduli at the surface and deep zone will be pursued in future studies, in order to obtain the information necessary to assess the spatial progression of OA changes in this model.

In conclusion, this study presents the first available data for changes in cartilage mechanics in the Hartley guinea pig model of OA; measures of the material moduli were obtained using an osmotic loading technique. These changes are likely associated with significant changes in cartilage load support and load distribution, consistent with increased matrix deformations upon loading and associated deleterious effects that may be involved in the progression of cartilage degenerative changes in the Hartley guinea pig. This characterization of material properties of cartilage in the guinea pig provides additional support for similarities in the pathogenesis of OA between this model and the human. Furthermore, these findings suggest that the osmotic loading method for material property determination may be a useful approach for quantifying cartilage function in small animal joints, such as the guinea pig, rat and mouse.

### Acknowledgements

This study was supported by funds from the NIH (R01-AR45644 and R29-AG15108) and from Pfizer Central Research, Pfizer, Inc. The authors wish to acknowledge the contributions of Dr. Daria A. Narmoneva (Massachusetts Institute of Technology) and Robert A. Skinner (University of Arkansas for Medical Sciences).

### References

1. Bendele AM, Hulman JF. Spontaneous cartilage degeneration in guinea pigs. *Arthritis Rheum* 1988; 31(4):561–5.
2. Bendele AM, White SL, Hulman JF. Osteoarthrosis in guinea pigs: Histopathologic and scanning electron microscope features. *Lab Animal Sci* 1989;39: 115–21.
3. de Bri E, Reinholt FP, Svensson O. Primary osteoarthrosis in guinea pigs: a stereological study. *J Orthop Res* 1995;13(5):769–76.
4. Hedlund H, de Bri E, Mengarelli-Widholm S, Reinholt FP, Svensson O. Ultrastructural changes in primary guinea pig osteoarthritis with special reference to collagen. *APMIS* 1996;104(5):374–82.
5. Wei L, Svensson O, Hjerpe A. Correlation of morphologic and biochemical changes in the natural history of spontaneous osteoarthritis in guinea pigs. *Arthritis Rheum* 1997;40(11):2075–83.
6. Jimenez PA, Glasson SS, Trubetsky OV, Haimes HB. Spontaneous osteoarthritis in Dunkin Hartley guinea pigs: histologic, radiologic, and biochemical changes. *Lab Animal Sci* 1997;47(6):598–601.
7. Kapadia RD, Badger AM, Levin JM, Swift B, Bhattacharyya A, Dodds, *et al.* Meniscal ossification in spontaneous osteoarthritis in the guinea-pig. *Osteoarthritis Cartilage* 2000;8(5):374–7.
8. Huebner JL, Otterness IG, Freund EM, Caterson B, Kraus VB. Collagenase 1 and collagenase 3 expression in a guinea pig model of osteoarthritis. *Arthritis Rheum* 1998;41(5):877–90.
9. Hayes WC, Mockros LF. Viscoelastic properties of human articular cartilage. *J Appl Physiol* 1971;31: 562–8.
10. Akizuki S, Mow VC, Muller F, Pita JC, Howell DS, Manicourt DH. Tensile properties of human knee joint cartilage: I. Influence of ionic conditions, weight bearing, and fibrillation on the tensile modulus. *J Orthop Res* 1986;4:379–92.
11. Roberts S, Weightman B, Urban J, Chappell D. Mechanical and biochemical properties of human articular cartilage in osteoarthritic femoral heads and in autopsy specimens. *J Bone Joint Surg* 1986;68-B: 278–88.
12. Guilak F, Ratcliffe A, Lane N, Rosenwasser MP, Mow VC. Mechanical and biochemical changes in the superficial zone of articular cartilage in canine experimental osteoarthritis. *J Orthop Res* 1994;12:474–84.
13. Setton LA, Mow VC, Muller FJ, Pita JC, Howell DS. Mechanical properties of canine articular cartilage are significantly altered following transection of the anterior cruciate ligament. *J Orthop Res* 1994;12: 451–63.
14. Setton LA, Mow VC, Howell DS. Mechanical behavior of articular cartilage in shear is altered by transection of the anterior cruciate ligament. *J Orthop Res* 1995; 13:473–82.
15. Sah RL, Yang AS, Chen AC, Hunt JJ, Halili RB, Yoshioka M, *et al.* Physical properties of rabbit articular cartilage after transection of the anterior cruciate ligament. *J Orthop Res* 1997;15:197–203.
16. Elliott DM, Guilak F, Vail TP, Wang JY, Setton LA. Tensile properties of articular cartilage are altered by meniscectomy in a canine model of osteoarthritis. *J Orthop Res* 1999;17:503–8.
17. LeRoux MA, Arokoski J, Vail TP, Guilak F, Hyttinen MM, Kiviranta I, *et al.* Simultaneous changes in the mechanical properties, quantitative collagen organization, and proteoglycan concentration of articular cartilage following canine meniscectomy. *J Orthop Res* 2000;18:383–92.
18. Bassar PJ, Schneiderman R, Bank RA, Wachtel E, Maroudas A. Mechanical properties of the collagen network in human articular cartilage as measured by osmotic stress technique. *Arch Biochem Biophys* 1998;351(2):207–19.
19. Narmoneva DA, Wang JY, Setton LA. Nonuniform swelling-induced residual strains in articular cartilage. *J Biomech* 1999;32:401–8.
20. Maroudas A. Balance between swelling pressure and collagen tension in normal and degenerate cartilage. *Nature* 1976;260:808–9.
21. Lai WM, Hou JS, Mow VC. A triphasic theory for the swelling and deformation behaviors of articular cartilage. *J Biomech Eng* 1991;113:245–58.
22. Narmoneva DA, Wang JY, Setton LA. A non-contacting method for material property determination for articular cartilage from osmotic loading. *Biophys J* 2001; 81:3066–76.
23. Flahiff CM, Narmoneva DA, Huebner JL, Kraus VB, Guilak F, Setton LA. Osmotic loading to determine the intrinsic material properties of guinea pig knee cartilage. *J Biomech* 2002;35(9):1285–90.
24. Narmoneva DA, Cheung HS, Wang JY, Howell DS, Setton LA. Altered swelling behavior of femoral cartilage following joint immobilization in a canine model. *J Orthop Res* 2002;20:83–91.

25. Eisenberg S, Grodzinsky A. Swelling of articular cartilage and other connective tissues: electromechanochemical forces. *J Orthop Res* 1985;3:148–59.
  26. Kiraly K, Lapvetelainen T, Arokoski J, Torronen K, Modis L, Kiviranta I, *et al.* Application of selected cationic dyes for the semiquantitative estimation of glycosaminoglycans in histological sections of articular cartilage by microspectrophotometry. *Histochem J* 1996;28:577–90.
  27. Lillie RD. *Histopathologic Technic and Practical Histochemistry*. 2nd edn. New York, NY: McGraw-Hill Book Company 1954.
  28. Martin I, Obradovic B, Freed LE, Vunjak-Novakovic G. Method for quantitative analysis of glycosaminoglycan distribution in cultured natural and engineered cartilage. *Ann Biomed Eng* 1999;27:656–62.
  29. Setton LA, Gu W, Lai MW, Mow VC. Predictions of swelling-induced pre-stress in articular cartilage. In: Selvadurai A, Ed. *Mechanics of Poroelastic Media*. Boston, MA: Kluwer Academic Publishers 1995; 299–320.
  30. Athanasiou KA, Zhu CF, Wang X, Agrawal CM. Effects of aging and dietary restriction on the structural integrity of rat articular cartilage. *Ann Biomed Eng* 2000;28:143–9.
  31. Carlson CS, Loeser RF, Purser CB, Gardin JF, Jerome CP. Osteoarthritis in cynomolgus macaques III: Effects of age, gender, and subchondral bone thickness on the severity of disease. *J Bone Min Res* 1996;11(9):1209–17.
  32. Mankin HJ, Dorfman H, Lippiello L, Zarins A. Biochemical and metabolic abnormalities in articular cartilage from osteoarthritic human hips. *J Bone Joint Surg* 1971;53A(3):523–37.
  33. Huebner JL, Hanes MA, Beekman B, TeKoppele JM, Kraus VB. A comparative analysis of bone and cartilage metabolism in two strains of guinea pig with varying degrees of naturally occurring osteoarthritis. *Osteoarthritis Cartilage* 2002;10:758–77.
  34. Kempson G. Mechanical properties and their relationship to matrix degradation. *Ann Rheum Dis* 2000; 34(Suppl):111–3.
  35. Elliott DM, Narmoneva DA, Setton LA. Direct measurement of the Poisson's ratio of human articular cartilage in tension. *J Biomech Eng* 2002;124:223–8.
  36. Hyttinen MM, Toyras J, Lapvetelainen J, Lindblom J, Prockop DJ, Li S-W, *et al.* Inactivation of one allele of the type II collagen gene alters the collagen network in murine articular cartilage and makes cartilage softer. *Ann Rheum Dis* 2001;60:262–8.
-